Supplementary Information

An In–Situ Growth Strategy for Core–Shell Cu_a–Zn_b–O_x/ZSM–5@S–1 to Boost Dimethyl Ether Synthesis from CO_2 Hydrogenation

Xinru Wang,† Fangzhou Wang,† Baorun Ma, Qihui Ding, Yanqin Wang,* and Xiaohui Liu*

Shanghai Key Laboratory of Functional Materials Chemistry, Research Institute of Industrial Catalysis, School of Chemistry and Molecular Engineering, East China University of Science and Technology, Shanghai 200237, China.

† These two authors contribute equally.

* Corresponding author: Dr. Xiaohui Liu, Email: xhliu@ecust.edu.cn, Dr. Yanqin Wang, Email: wangyanqin@ecust.edu.cn.

Experimental section

Materials

Sodium aluminate ($NaAlO_2$, 99%), and tetraethyl orthosilicate (TEOS, 99.9%) were purchased from Sinopharm Chemical Reagent Co., Ltd. Tetrapropylammonium hydroxide (TPAOH, 25 wt.% in water) was purchased from Saen Chemical Technology Co., Ltd. Copper nitrate trihydrate ($Cu(NO_3)_2 \cdot 3H_2O$, 99.0%), and zinc nitrate hexahydrate ($Zn(NO_3)_2 \cdot 6H_2O$, 99.0%) were purchased from Shanghai Adamas Reagent Co., Ltd. All chemicals were used without further purification. The feed gas mixture (25% CO_2 + 75% H_2) was supplied by Air Liquid Co., Ltd.

Synthesis of the catalysts

ZSM–5 zeolite was hydrothermally synthesized following the procedure described earlier.[1, 2] Briefly, 0.207 g $NaAlO_2$ was dissolved in a mixed solution of 10.84 g TPAOH and 12.86 g ultra-pure water, targeting a Si/Al molar ratio of 37. The mixture was stirred for 2 h at room temperature, after which 6.94 g TEOS was added to the mixture. The resultant product was stirred for an additional 6 h at room temperature before being transferred to a Teflon-lined autoclave for crystallization at 170°C for 72 h. The solid sample was recovered by repeated centrifugation and washing until the washing solution reached a pH of 7, then dried and calcined at 600 °C for 5 h. The calcined sample was subsequently subjected to ion exchange by stirring in a 1 mol/L NH_4Cl solution at a mass ratio of 1:30 at room temperature. Finally, the filtered solid sample was calcined again at 600 °C for 5 h.

Pure-silica MFI type Silicalite–1 (S–1) zeolite was hydrothermally synthesized following the procedure described earlier.[3, 4] Briefly, TEOS, TPAOH and ultra-pure water were mixed in a molar ratio of 1:0.4:35. Weigh 13.0 g of TPAOH and mix it with 15.0 g of ultra-pure water, then add 8.3 g of TEOS dropwise. The resulting mixture was stirred at room temperature for 6 h. The resulting homogeneous solution was transferred into a Teflon–lined autoclave and crystallized at 170 °C for 72 h. The solid sample was collected by repeated centrifugation and washing until the washing solution reached a pH of 7, dried, and finally calcined at 600 °C for 5 h.

A series of Cu_a–Zn_b–O_x/ZSM–5 and Cu_a–Zn_b–O_x/S–1 catalysts with different Cu and Zn loadings were prepared by a sequential wet impregnation method. Briefly, specified amounts of $Cu(NO_3)_2 \cdot 3H_2O$ were dissolved in 0.6 g of deionized water and then mixed with 1.0 g of ZSM–5 or S–1 support. The mixture was thoroughly blended, sonicated for 15 min, dried at 60 °C for 12 h, increased from room temperature to 600 °C at a heating rate of 1 °C/min and calcined at 600 °C for 5 h to obtain the Cu_a–

O_x/ZSM–5 or Cu_a–O_x/S–1 materials. These monometallic catalysts were subsequently used as supports for the introduction of zinc via the same impregnation procedure, using $Zn(NO_3)_2 \cdot 6H_2O$ as the precursor. After the same procedures, the bimetallic Cu_a–Zn_b–O_x/ZSM–5 and Cu_a–Zn_b–O_x/S–1 catalysts were obtained, where a and b denote the theoretical weight percent of Cu and Zn, respectively.

The preparation method of the core–shell Cu_a–Zn_b–O_x/ZSM–5@S–1–n catalyst is described as follows: First, TPAOH, TEOS and ultra-pure water were mixed at the same molar ratio as that for S–1 synthesis and stirred for 6 h. A certain mass of the precursor Cu_a–Zn_b–O_x/ZSM–5 was then added to the mixture, which was subsequently stirred in a water bath at 60 °C until the solution was completely dried. The solid was ground into powder and transferred into a Teflon–lined autoclave. A small amount of TPAOH solution was added to infiltrate the powder, followed by crystallization at 170 °C for 48 h to realize in–situ growth of S–1 and formation of the core–shell structured catalyst. After sequential procedures of cooling, washing, drying, and calcination, the Cu_a–Zn_b–O_x/ZSM–5@S–1–n catalyst was obtained. Herein, the subscripts of a and b in Cu_a–Zn_b–O_x/ZSM–5@S–1 represent the theoretical loading amounts of Cu and Zn on ZSM–5, respectively, "n" represents the theoretical mass ratio of S–1 to ZSM–5 in the catalyst (n = 1, 2, 3), which was determined by the mass of the silicon source (TEOS) and the mass of ZSM–5 in the precursor. Unless otherwise specified, Cu_a–Zn_b–O_x/ZSM–5@S–1 refers to the catalyst with n = 2. For comparison, the Cu_a–Zn_b–O_x/(ZSM–5@S–1) catalyst was also prepared. Specifically, the core–shell structured support ZSM–5@S–1 was first synthesized via the same method mentioned above, and then Cu and Zn metals were loaded onto the support through an impregnation method.

Catalyst Characterization

Powder X–ray diffraction (XRD) patterns were recorded on a Rigaku Max 2550VB diffractometer equipped with a Cu Kα radiation source (λ=1.5406 Å) operating at 40 kV and 40 mA. The measurements were performed over a 2θ range of 5° to 75° at a scanning rate of $2° \cdot min^{-1}$ to assess the crystallinity and phase composition of the as–synthesized and reduced catalysts.

N_2 physisorption measurements were performed at 77 K on a Micromeritics ASAP 2020M analyzer to determine the textural properties of the catalysts. Prior to analysis, each sample was degassed under vacuum at 200 °C for 6 h to remove adsorbed contaminants. The Brunauer–Emmett–Teller (BET) method was applied to calculate the specific surface area, while the pore size distribution of the zeolite component was derived using density functional theory (DFT) models based on the adsorption branch.

The dead volume of the sample tube was calibrated with helium before measurement.

The elemental composition of the catalyst was determined by inductively coupled plasma optical emission spectrometry (ICP–OES) using an Agilent 725ES instrument.

Aberration–corrected scanning transmission electron microscopy (AC–STEM) characterization was carried out on a Thermo Fisher Talos F200X microscope operated at 200 kV. The instrument is equipped with four in–column Super–X detectors for energy–dispersive X–ray spectroscopy (EDS). For AC–HAADF and AC–BF imaging, a convergence semi–angle of 11 mrad was used, with collection semi–angles of 59–200 mrad. For analysis, the catalyst powder was finely ground, dispersed in anhydrous ethanol, and ultrasonicated for 30 min. A droplet of the suspension was deposited onto an ultrathin Mo grid and dried; this process was repeated three times to ensure adequate loading.

H_2–temperature–programmed reduction (H_2–TPR) was conducted on a Vodo VDsorb–91i analytical system equipped with a thermal conductivity detector (TCD). Prior to measurement, the catalyst was pretreated under an Ar flow at high temperature for 1 h. The TPR profile was recorded while heating the sample from ambient temperature to 400 °C at a rate of 10 °C·min^{-1} under a 10 vol% H_2/Ar flow. The H_2 consumption of each sample was determined by integrating the corresponding peaks in the H_2–TPR profiles and applying a pre–established calibration curve relating peak area to H_2 uptake. The reduction degree was then calculated as the ratio of the experimental H_2 consumption to the theoretical amount required for complete reduction of the metal species to their metallic state.

NH_3–temperature–programmed desorption (NH_3–TPD) was performed using an automated chemisorption analyzer (Tianjin Pengxiang Co., Ltd.) with a TCD. Approximately 50 mg of catalyst (40–60 mesh) was first pretreated at 500 °C for 1 h under N_2 flow (20 mL·min^{-1}) and then cooled to 90 °C. The sample was exposed to NH_3 at 90 °C for 30 min, followed by flushing with N_2 to remove physisorbed NH_3 and stabilize the baseline. The temperature was then ramped to 600 °C at 10 °C·min^{-1} under N_2, and the desorption signal was recorded.

X–ray photoelectron spectroscopy (XPS) analysis was performed on a Thermo Scientific Escalab 250 Xi spectrometer using monochromated Al Kα radiation ($h\nu$ = 1486.7 eV, 225 W) with a base pressure of 10^{-9} torr. All binding energies were referenced to the C 1s peak at 284.8 eV, and spectral fitting was conducted using the Avantage software.

CO_2–temperature–programmed desorption (CO_2–TPD) was carried out on a Vodo

VDsorb–91i apparatus equipped with a TCD. The catalyst was first reduced in a 10 vol% H_2/Ar flow at 400 °C for 1 h, cooled to 50 °C, and then exposed to CO_2 for 30 min. After purging with Ar for 30 min to remove physisorbed CO_2 and stabilize the baseline, the temperature was increased to 600 °C at a rate of 10 °C·min^{-1} under Ar flow, and the desorption profile was recorded.

CO diffuse reflectance infrared Fourier transform spectroscopy (CO–DRIFTs) were performed using a Thermo Fisher Nicolet iS50 spectrometer in the range from 600 to 4000 cm^{-1} equipped with a liquid nitrogen–cooled MCT/A detector and a Harrick in situ reaction cell. Spectra were collected in the range of 600–4000 cm^{-1} with a resolution of 4 cm^{-1}, accumulating 32 scans at an interval of 0.5 cm^{-1}. A KBr beamsplitter and a ZnSe window were used for optical alignment. Prior to CO adsorption, the sample was purged under Ar at the target temperature for 30 min. The atmosphere was then switched to a 1% CO/Ar mixture for adsorption until saturation, followed by Ar purging to remove gaseous and weakly adsorbed CO before collecting the final spectrum.

Catalyst Performance Testing

The catalytic performance for CO_2 hydrogenation to DME was evaluated in a high–pressure fixed–bed reactor. Catalyst particles (40–60 mesh) were loaded into a 6 mm stainless–steel tubular reactor with a catalyst mass of 0.30 g. The catalyst was placed in the middle section of the reactor, and the voids at both ends were filled with quartz sand. Prior to reaction, the catalyst was reduced in situ under pure H_2 (30 mL·min^{-1}) at 400 °C at a heating rate of 10 ℃/min and atmospheric pressure for 2 h. After the reduction was completed, the temperature was lowered to 260 ℃ under a H_2 atmosphere, and then the gas was switched to the reaction gas H_2/CO_2 volume ratio of 75:25. Standard reaction conditions were maintained at 3 MPa, 260 °C, and a weight hourly space velocity (WHSV) of 6000 mL·g_{cat}^{-1}·h^{-1}, unless otherwise stated. The effluent stream was directed via a heated transfer line (180 °C) to an online gas chromatograph for product analysis. CO and CO_2 were separated using a TDX–01 packed column (3 mm × 1 m) and detected by a thermal conductivity detector with H_2 as the carrier gas. Hydrocarbons, methanol, and DME were separated using a Restek RT–Q–BOND capillary column (0.25 mm × 40 m) and quantified with a flame ionization detector. The formulas used for calculating CO_2 conversion, product selectivity, and reaction rate are provided below.

$$Conv.(CO_2) = \frac{\left[X(CO) + X(CH_4) + X\left(C_2^+\right) + X(CH_3OH)\right] \times f_{out}}{X(CO2)_{in} \cdot f_{in}} \times 100\%$$

Formula (2-1)

$$S(product) = \frac{X(product)}{X(CO) + X(CH_4) + X(C_2^+) + X(CH_3OH)} \times 100\%$$

Formula (2-2)

$$r(product) = \frac{X(product) \times f_{out}}{g_{cat}}$$

Formula (2-3)

$$Carben\ balance = \frac{F_{out} \times (y_{CO_2,out} + y_{CO,out} + y_{CH_4,out} + y_{CH_3OH,out} + 2y_{DME,out})}{F_{in} \times y_{CO_2,in}} \times 100\%$$

Formula (2-4)

$$STY_{DME} = \frac{F_{CO2} \times y_{CO2} \times X_{CO2} \times S_{DME} \times 60}{22400 \times m_{cat} \times \omega_{Cu}} \times 2 \times 1000$$

Formula (2-5)

in where, Conv.(CO_2): CO_2 conversion, %; X(product): molar concentration of gas phase components, %; Product: CO, CH_4, CH_3OH, and C_2^+ (C2–C5); f_{in} and f_{out}: gas flow rate, mmol/h; S(product): product selectivity, %; g_{cat}: catalyst mass, g; r(product): reaction rate, mmol/g_{cat}/h; F represents the total flow rate (mL/min) and y represents the volume fraction of each component; STY_{DME}: mmol/g_{Cu}/h; F_{CO2} is the flow rate of CO_2, mL/min; y_{CO2} is the volume fraction of CO_2 in the feed gas; X_{CO2} is the conversion of CO_2; S_{DME} is the selectivity of DME; m_{cat} is the mass of the catalyst, g; and ω_{Cu} is the Cu content in the catalyst, g_{Cu}/g_{cat}.

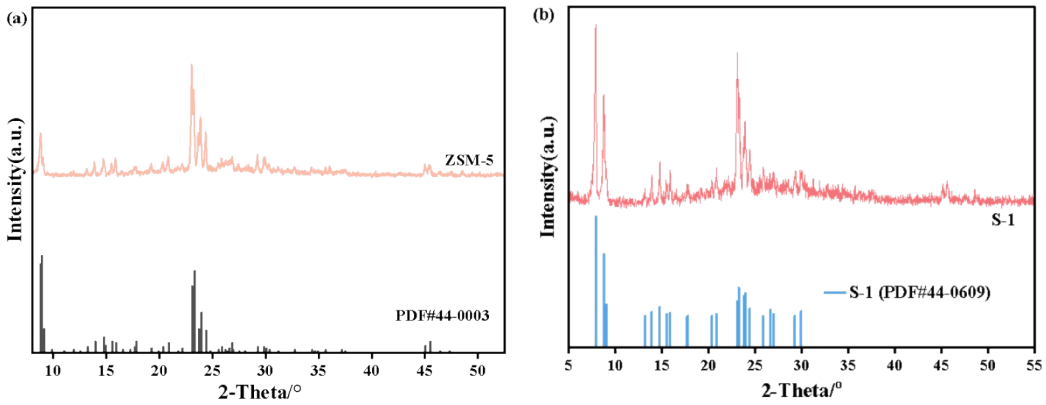

Figure S1. XRD diffraction patterns of (a) ZSM–5 and (b) S–1 supports.

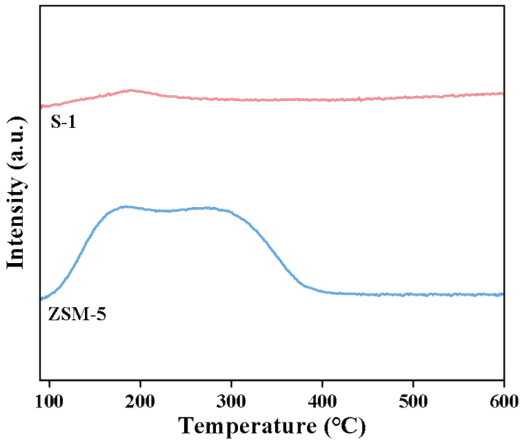

Figure S2. NH_3–TPD of ZSM–5 and S–1 supports.

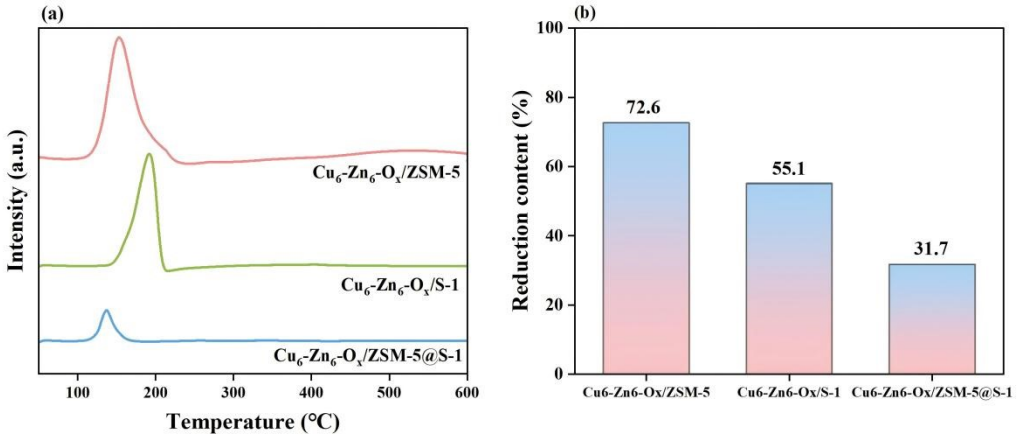

Figure S3. (a) H_2–TPR and (b) reduction degree of different catalysts.

Table S1. Structural parameters and metal content of various samples.

Catalysts	Surface area ($m^2\ g^{-1}$)	Pore size (nm)	Zn[a] (wt.%)	Cu[a] (wt.%)
ZSM–5	353	1.9	--	--
S–1	412	2.5	--	--
Cu_6–Zn_6–O_x/ZSM–5	228	2.0	5.6	5.6
Cu_6–Zn_6–O_x/S–1	344	2.4	6.0	6.0
Cu_6–Zn_6–O_x/ZSM–5@S–1	392	2.5	2.1	2.0
Cu_6–Zn_6–O_x/(ZSM–5@S–1)	381	2.2	5.8	6.0

a: Data determined by ICP–OES.

Table S2. Catalytic performance of CO_2 hydrogenation to dimethyl ether on the different catalysts.

Entries	Catalysts	CO_2 Conv.	Selectivity (mol %)				Carbon balance	STY_{DME}
		(%)	CO	CH_4	CH_3OH	DME	(%)	(mmol/g_{Cu}/h)
1	Cu_6–Zn_6–O_x/ZSM–5	0.7	51.3	1.4	24.7	22.2	96.8	3.47
2	Cu_6–Zn_6–O_x/S–1	5.2	78.4	0.1	21.5	--	98.5	--
3	Cu_6–Zn_6–O_x/ZSM–5@S–1	6.8	20.9	0.1	5.4	73.6	97.6	335.14
4	Cu_6–Zn_6–O_x/(ZSM–5@S–1)	3.5	25.2	0.5	3.3	71.0	98.9	55.47

Reaction conditions: Gas flow rate 30 mL/min, 0.3 g catalyst, 260 ℃, 3.0 MPa.

Table S3. Catalytic performance of CO_2 hydrogenation to dimethyl ether on the Cu_6–Zn_6–O_x/ZSM–5@S–1 catalysts with different S–1 contents.

Entries	Catalysts	CO_2 Conv. (%)	Selectivity (mol %)				Zn wt.%	Cu wt.%
			CO	CH_4	CH_3OH	DME		
1	Cu_6–Zn_6–O_x/ZSM–5@S–1–1	4.2	20.0	0.3	7.2	72.5	3.0	3.1
2	Cu_6–Zn_6–O_x/ZSM–5@S–1–2	6.8	20.9	0.1	5.4	73.6	2.0	2.0
3	Cu_6–Zn_6–O_x/ZSM–5@S–1–3	4.2	21.6	0.4	8.9	69.1	1.4	1.3

Reaction conditions: Gas flow rate 30 mL/min, 0.3 g catalyst, 260 ℃, 3.0 MPa.

Note: The performance of Cu_6–Zn_6–O_x/ZSM–5@S–1 catalysts, synthesized with different S–1/ZSM–5 coating mass ratios, exhibits an optimal shell thickness was identified at n=2. As the coating mass ratio increases, the CO_2 conversion first increases and then decreases, while the DME selectivity remains relatively stable.

Table S4. Catalytic performance of CO_2 hydrogenation to dimethyl ether on the Cu_a–Zn_b–O_x/ZSM–5@S–1 catalysts with various Cu and Zn loadings.

Entries	Catalysts	CO_2 Conv. (%)	Selectivity (mol %)			
			CO	CH_4	CH_3OH	DME
1	Cu_6–Zn_3–O_x/ZSM–5@S–1	5.9	34.7	0.1	2.8	62.4
2	Cu_6–Zn_6–O_x/ZSM–5@S–1	6.8	20.9	0.1	5.4	73.6
3	Cu_6–Zn_9–O_x/ZSM–5@S–1	11.3	11.7	0.1	6.3	81.9
4	Cu_9–Zn_9–O_x/ZSM–5@S–1	12.0	13.2	0.4	11.2	75.2

Reaction conditions: Gas flow rate 30 mL/min, 0.3 g catalyst, 260 ℃, 3.0 MPa.

Table S5. Catalytic performance of CO_2 hydrogenation to dimethyl ether on the Cu_6–Zn_9–O_x/ZSM–5@S–1 catalyst under different reaction conditions.

Catalysts	Temperature (°C)	Pressure (MPa)	WHSV (mL/g_{cat}/h)	CO_2 Conv. (%)	Selectivity (mol %)			
					CO	CH_4	CH_3OH	DME
Cu_6–Zn_9–O_x/ZSM–5@S–1	180	3.0	6000	2.2	6.8	0.0	57.5	35.7
	220	3.0	6000	6.3	16.6	0.2	21.3	61.9
	260	3.0	6000	11.3	11.7	0.1	6.3	81.9
	300	3.0	6000	20.0	44.6	1.7	3.0	50.7
	260	3.0	3000	15.1	11.7	0.1	8.5	79.7
	260	3.0	12000	7.5	10.1	0.1	27.3	62.5
	260	3.0	18000	4.6	11.4	0.1	43.4	45.1
	260	5.0	3000	22.3	11.5	0.2	2.4	85.9

Table S6 Surface acidity analysis of different catalysts.

Catalysts	Total acid amount	Distribution of acid strength			Percent of acid strength (%)		
	(mmol NH_3 g^{-1})	Weak	Medium	Strong	Weak	Medium	Strong
Cu_6–Zn_6–O_x/ZSM–5	0.60	0.22	0.38	--	36.0	64.0	--
Cu_6–Zn_6–O_x/S–1	0.28	0.10	0.15	0.03	34.6	54.5	10.9
Cu_6–Zn_6–O_x/ZSM–5@S–1	0.37	0.06	0.17	0.14	16.3	45.6	38.1

Table S7. H_2 consumption and reduction degree of Cu in the different catalysts obtained from H_2-TPR[a].

Catalysts	T (℃)	H_2 (mmol)	Reduction degree (%)
Cu_6–Zn_6–O_x/ZSM–5	191	0.064	72.6
Cu_6–Zn_6–O_x/S–1	152	0.052	55.1
Cu_6–Zn_6–O_x/ZSM–5@S–1	130	0.010	31.7

a: 100 mg catalysts. The reaction degree of Cu is determined based on the actual Cu content measured by ICP.

Reference

1. R. Van Grieken, J. L. Sotelo, J. M. Menéndez and J. A. Melero, *Microporous and Mesoporous Materials*, 2000, **39**, 135-147.
2. D. P. Serrano, J. Aguado, G. Morales, J. M. Rodríguez, A. Peral, M. Thommes, J. D. Epping and B. F. Chmelka, *Chem. Mat.*, 2009, **21**, 641-654.
3. Y. Q. Xie, X. J. Meng, S. Gao, Z. B. Wu and F. S. Xiao, *Microporous and Mesoporous Materials*, 2022, **346**, 7.
4. C. S. Cundy and P. A. Cox, *Microporous and Mesoporous Materials*, 2005, **82**, 1-78.